Applied Biological Research 28(1): 50-61; (2026)
DOI: 10.48165/abr.2026.28.01.6

BIOGENIC SYNTHESIS AND CHARCTERIZATION OF SILVER NANOPARTICLES FROM *Vitex leucoxylon* BARK EXTRACT AND ITS MEDICAL APPLICATIONS

Dickson Kayabu[1], Patrick Francis Kimariyo[2], Rajesh Babu Yerramneediand[3], and S.B. Padal[3]

[1]*Department of Biotechnology,* [3]*Department of Botany, College of Science & Technology, Andhra University, Visakhapatnam – 530 003, Andhra Pradesh (India)*
[2] *Department of Science and Laboratory, Dar es Salaam Institute of Technology (DIT), P.O. Box 2958, Dar es salaam (Tanzania)*
*e-mail: *dicksonkayabu@gmail.com*

(Received 13 November, 2024; accepted 18 January, 2026)

ABSTRACT

Phytsyhthesized nanoparticles from different medicinal plants are currently exploited for large scale biomedical applications. The biosynthesis of silver nanoparticles (AgNPs) was carried out by using the aqueous extract of *Vitex leucoxylon* bark and its properties evaluated by UV-vis spectroscopy, FTIR, and XRD analysis. Also, the antimicrobial, cytotoxic, and antioxidant properties of biosynthesized AgNPs were assessed using standard methods. A characteristic surface plasmon resonance peak at 435 nm, observed in UV-visible spectrum, confirmed the formation of *V. leucoxylon* bark aqueous extract-based AgNPs (Vl-AgNP). The peaks in FTIR analysis showed the presence of several organic constituents that acted as capping and reducing substances. XRD measurements confirmed that Vl-AgNPs were crystalline face-centred cubic structures. DLS analysis of synthesized AgNPs showed a mean hydrodynamic diameter of 177.6 nm with low polydispersity (0.090) and high colloidal stability (−82.8 mV). SEM-EDX analysis showed it to be uniformly distributed Vl-AgNP, while TEM analysis revealed spherical nanoparticles of 50 to 64 nm size. The Vl-AgNPs demonstrated substantial anti-bacterial activity towards human pathogenic bacteria and strong antioxidant activity in dose-dependent manner with maximum inhibition against *Escherichia coli*. Antioxidant activity showed dose-dependent radical scavenging activity, reaching 77.42 ± 1.25% in DPPH assay at 100 µg mL^{-1}, while FRAP analysis demonstrated moderate reducing power. *In vitro* cyto-toxicity studies using the MTT assay revealed dose-dependent inhibition of HeLa cells line with an IC_{50} value of 74.38 µg mL^{-1}. These findings confirm the notable bioactivity of Vl-AgNPs, highlighting their potential biomedical applications.

Keywords: Antibacterial, anticancer, antioxidant, *Vitex leucoxylon,* silver nanoparticles

INTRODUCTION

Nanotechnology is a captivating field of science that is rapidly influencing the several facets of human existence. Nanoparticles (NPs) are the materials having diameters in the range of 1 to 100 nm (Raja *et al*., 2024). NPs have attracted significant interest owing to their beneficial uses in several disciplines, such as health science, material science, and natural science. The nanoparticle synthesis involves biological, chemical, and physical techniques. Traditionally, methods such as laser ablation, ball milling, chemical reduction, the sol-gel process, and co-precipitation were used for the fabrication of NPs. Nevertheless, these techniques are expensive and eco-unfriendly.

Alternatively, the biological method is the most affordable option for the manufacture of nanoparticles because it is eco-friendly and cost-effective (Ahmed *et al*., 2016).

Silver nanoparticles (AgNPs) are among the most extensively studied inorganic nanoparticles due to their efficacy in eradicating many bacterial strains, their chemical stability, catalytic properties, and low toxicity at minimal concentrations. They not only can combat bacteria, fungi, and viruses but also have the properties that fight cancer, reduce swelling, and help wounds heal (Barabadi *et al*., 2020). They have biological impacts because they can break down microbial membranes, generate reactive oxygen species, interact with proteins and DNA, and stop important metabolic processes (Chahardoli *et al*., 2022).

Plants possess diverse biomolecules, including terpenoids, alkaloids, phenolics, and proteins, distributed across the numerous plant parts such as stems, roots, barks, leaves, and fruits. These biomolecules can facilitate the synthesis of AgNPs by reducing Ag+ to Ag° (Jalilian *et al*., 2020). In Indian medicine, herbal extracts have traditionally been used to treat a range of ailments, including infections, inflammation, fever, pain, digestive issues, and skin diseases (Manisha *et al*., 2025). Consequently, nanoparticles generated from such herbal extracts may function as bactericidal agents, antioxidants, and anticancer compounds. *Vitex leucoxylon* is a medicinal plant from the Lamiaceae family, predominantly found in India and Sri Lanka. It has been utilized for an extended period to address many diseases (Muthukrishnan *et al*., 2025). The bark contains secondary metabolites such as phenolics, flavonoids, and terpenoids, which possess antibacterial, antioxidant, anti-inflammatory, neuroprotective, and antidepressant properties (Vinothkanna *et al*., 2024). *V. leucoxylon* has potential medicinal applications; yet, its use in nanotechnology, particularly for the green synthesis of silver nanoparticles has less been exploited. The phytogenic production of AgNPs presents a potential method that integrates plant bioactivity with improved nanoscale effectiveness. The present study was aimed to synthesize silver nanoparticles by using the bark extract of *Vitex leucoxylon*, comprehensively characterize its physicochemical properties and evaluate its anti-bacterial, antioxidant, and cytotoxic activities using the HeLa cell line.

MATERIALS AND METHODS

Collection of Vitex leucoxylon

Healthy barks of *Vitex leucoxylon* plant (Fig. 1) were collected in August 2025 from the Vanjangi Hills Trek Forest (18°00′08.50″ N, 82°29′10.61″ E) Alluri Sitharama Raju district, Andhra Pradesh, India. The identification and authentication of plant materials was done by the Department of Botany, Andhra University, and a reference voucher specimen was deposited in the Andhra University Herbarium vide No. 25439 AUV.

Aqueous plant extract preparation

Vitex leucoxylon barks were thoroughly cleaned under running tap water and shade-dried for 21 days at 30 ± 2°C. The dried plant material was ground using a mechanical grinder at 5000 rpm for 5 min and sifted through a 60 µm sieve to obtain bark powder. Bark powder (10 g) was added to the demineralized water to make a final volume of 100 mL. The mixture was boiled at 80°C for 30 min and then filtered using Whatman No. 1 filter paper to obtain the aqueous extract (Fig. 2A). The filtered extract was stored at 4°C in a 250 mL conical flask for further studies.

Fig. 1: *Vitex leucoxylon* barks

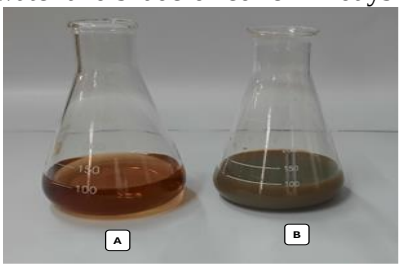

Fig. 2: A) *V. leucoxylon* aqueous bark extract; B) phyto-synthesized AgNPs after 24 h of incubation

Phytochemical analysis

A phytochemical screening of *V. leucoxylon* was conducted to qualitatively investigate numerous bioactive substances with no nutritional value found in the aqueous extract of *V, leucoxylon* bark. Phytochemical screening of bark extract was carried out using standard qualitative methods described by Harborne (1998).

Phytosynthesis of AgNPs

The biosynthesis AgNPs using *V. leucoxylon* bark extract was conducted as per the method described by Chinnasamy *et al*. (2024) with slight modification. Briefly, 10 mL of water-based extract was dissolved in 90 mL of 1 mM silver nitrate ($AgNO_3$) solution in a 250 mL conical flask. The mixture was heated for 2 h at 70ºC on a hot plate magnetic stirrer (model: GMS-10, Garg India) with continuous stirring at the rate of 450 rpm, followed by a 24 h incubation at 37ºC. The change in colour indicated the successful synthesis of AgNPs (Fig. 2). The synthesis of AgNP was further validated by ultraviolet-visible spectroscopic analysis (Khutade *et al.,* 2025). The AgNPs were collected after centrifugation at 18000 rpm for 20 min, washed three times with demineralized water, air dried, and stored for subsequent characterization and evaluation of antibacterial, anticancer, and antioxidant potential.

UV-Vis spectroscopy analysis: The UV-Vis spectroscopy analysis of both bark extract and synthesized AgNPs was performed by using UV-vis spectrometer (UV-1900i, Shimadzu Japan). The resolution of UV-visible spectrometer was set at 1 nm and 800-350 nm scan range (Vinothkanna *et al.*, 2024). Silver nitrate solution was used as blank.

FTIR spectroscopy analysis: The AgNPs and dried plant extract were separately mixed with spectroscopic-grade KBr powder (2 mg sample 100 mg^{-1} KBr) and pressed into pellets. The FTIR spectra were recorded using a compact FTIR spectrometer (Alpha II spectrometer, Bruker Germany) in the infrared range of 4000-500 cm^{-1}.

XRD characterization: The crystalline nature of AgNPs was analysed by using X-ray diffraction (Jalilian *et al.,* 2020). Diffraction patterns were obtained using a computer-controlled X-ray diffractometer (D8 Advance, Bruker Germany) employing Cu Kα radiation (λ = 1.5418 Å). The data were recorded over a 2θ range of 20-80° using a nickel filter. The crystallite size of AgNPs was calculated using the Debye–Scherrer equation to confirm their crystalline characteristics.

Particle size and Zeta potential analysis: Particle size distribution and Zeta potential were measured using a SZ-100 particle size analyser (Horiba, Japan). For analysis, 1 mg AgNPs was dispersed in 10 mL demineralized water by vortex mixing, then followed by ultra-sonication at 40 kHz for 10 min to ensure uniform dispersion. The suspension was transferred to a 10 mm path-length transparent cuvette for particle size analysis (Kumar *et al*., 2020), while the same sample was used for zeta potential measurement in a 6-mm gold-coated cuvette.

FE-SEM and EDX analysis: A field-emission scanning electron microscope (FE-SEM; JSM-7610F, Jeol Japan) with an energy-dispersive X-ray (EDX) detector was used to look at the surface morphology of Vl-AgNPs. The FE-SEM worked at an accelerating voltage of 15 kV. The associated EDX equipment, which can detect levels as low as 0.5%, was used to analyse the elemental composition (Khan *et al.*, 2021).

TEM analysis: In addition to Zeta potential evaluation of *V. leucoxylon* bark-based AgNPs (Al-AgNPs), the shape and size was examined by using a transmission electron microscope (Hillsboro model, Philips GM-30), operating at a voltage of 120 kV (Gengan *et al*., 2013). The synthesized Al-AgNPs were sonicated at 40 kHz for 5 min after being suspended in a multiple quantum well. An infrared lamp was used to evaporate the solvent after a (50 µL) drop of resulting solution was put on a copper mesh grid coated carbon. Particle morphology, size, and size distribution were evaluated.

Antibacterial activity of Vl-AgNPs

Agar plate method was employed to assess the bacteria-inhibiting activity of phytosynthesized AgNPs (Alzahrani *et al.*, 2021). The four human pathogenic bacteria *viz*., Gram-positive (*Bacillus coagulans* MTCC-13124 and *Staphylococcus aureus* MTCC-3160) and Gram-negative (*Escherichia coli* MTCC-443 and *Pseudomonas aeruginosa* MTCC-6363) were procured from the Institute of Microbial Technology, India. Bacteria were sub-cultured in LB broth and incubated at 37°C for 24 h. Thereafter, each cultured bacterium was made to the standard concentration (0.5 McFarland). After spreading bacterial cultures on the plates containing MH-agar, punched wells were made by employing agar wells puncher. Wells were filled with various Al-AgNP concentrations and incubated for 24 h at 37°C. Finally, the areas of inhibitions were determined (Dua *et al.*, 2023).

Minimum inhibitory concentration

B. coagulans MTCC-13124, *S. aureus* MTCC-3160), *P. aeruginosa* MTCC-6363 and *E. coli* MTCC-443) bacterial pathogens were used to assess minimum inhibitory concentration (MIC) as per broth dilution method (Wiegand *et al.*, 2008). For bacterial strains, Mueller-Hinton (MH) broth was used. Each tube of sterile MH broth was inoculated with 5 µL (5×10^8 CFU mL^{-1}) of fresh cultures. Then various quantities of Al-AgNPs (5-100 µg mL^{-1}) were added. Broth and inoculum served as positive control broth and Al-AgNPs and broth alone served as negative control. The tubes containing bacteria were cultured at 37°C for 24 h. The absorbance was measured at 600 nm using UV-vis spectrophotometer (Shimadzu UV-1800, Japan).

Minimum bactericidal concentration

The minimum bactericidal concentration (MBC) was calculated by using the traditional method (Chinnasamy *et al.*, 2024). In this method, MIC dilutions were sub-cultured on sterile MH agar plates and incubated for 24 h at 37°C to obtain MBC value. MBC is the minimum amount of nanoparticles needed to eradicate the test bacterium. Biosafety cabinets were used for all experiments. Comparing the MBC value with negative control (no treatment) revealed a correlation with the concentration at which 100% of bacterial growth was inhibited.

In vitro antioxidant activity of Vl-AgNP

DPPH radical scavenging assay: With a minor modification, the method of Cuendet *et al.*, 1997) was used to assess Vl-AgNP's capacity to capture DPPH radicals. In this experiment, 1 mL DPPH solution in methanol (0.1 mM) was added to 2 mL Vl-AgNPs and incubated at 37°C for 30 min prior to recording absorbance at 517 nm against control by using UV-visible spectrophotometer. Absorbance of test samples and controls were compared to find the percentage of inhibition. Subsequent formula was applied to find the inhibition percentage (I) as radical scavenging activity:

$$\text{Percentage of inhibition (I)} = \frac{(\text{Absorbance of Control} - \text{Absorbance of Test})}{(\text{Absorbance of control} \times 100)}$$

FRAP assay: The technique outlined by Manimaran *et al.* (2021) was used to analyse the ferric-reducing antioxidant power (FRAP) of Vl-AgNPs. The complex compound's absorbance (ferric-tripyridyltriazine) formed from coloured form of iron (II) with antioxidants was measured using this technique. For this, 2.5 mL of 1% potassium ferricyanide was combined with varying amounts of synthetic Vl-AgNPs (10 - 50 µg mL^{-1}) and acetate buffer (pH 3.6, 2.5 mL, 0.3 M). After 30 min incubation at 37°C, the mixture was supplemented with 2.5 mL of 10% trichloroacetic acid. Thereafter, distilled water and 1% iron (III) chloride with volume of 2.5 and 0.5 mL, respectively, were added to the solution. The absorbance was noted at 630 nm. A higher reducing power is shown by an increase in the absorbance of the mixture reacting. As the standard, ascorbic acid was used.

Determination of cytotoxic activity of Vl-AgNPs using MTT assay

The cancer cell lines of HeLa were acquired from the National Center for Cell Science India and the inhibitory effects of AgNPs synthesized from *V. leucoxylon* against HeLa cell lines were assessed by MTT assay (DeGraff and Mitchell, 1987). The dehydrogenase enzyme in mitochondria of

healthy cells transforms mitochondria of healthy cells from a yellow tetrazolium salt, MTT [3-(4,5-dimethylthiazol-2-yl)-2,5-diphenyltetrazolium bromide] into a violet-coloured formazan product. In a 96-wells plate, the cells were subjected to varying concentrations of Vl-AgNPs (12.5-200 µg mL^{-1}) and incubated for 24 h. Following incubation, the culture media was discarded, and 15 µL MTT solution was introduced to each well. After a 3-h incubation in dark, the MTT was removed, and the resultant formazan crystals were dissolved in DMSO (100 µL $well^{-1}$). The absorbance was measured at 570 nm using an ELISA microplate reader. The percent cell viability was determined using the following formula and expressed as IC_{50}:

$$\text{Percentage of growth inhibition} = \frac{\text{OD of test}}{\text{OD of control}} \times 100$$

Statistical analysis

All experiments were performed in triplicate (n = 3), and data are presented as mean ± standard deviation (SD). Statistical analysis was carried out using GraphPad Prism 9 software. Differences between control and treated groups were analysed using two-way analysis of variance (ANOVA) with Tukey's test. A value of $p < 0.05$ was considered statistically significant.

RESULTS AND DISCUSSION

Phytogenic synthesis of AgNPs

For fabrication of *V. leucoxylon*-based silver nanoparticles (Vl-AgNPs), the bark extract of *V. leucoxylon* (10 mL) was used to reduce 1 mM $AgNO_3$ (90 mL) at 70°C under continuous stirring. The colour initially appeared brown which gradually turned dark brown within the first 2 h and subsequently the colour changed to greenish brown after incubation for 24 h at room temperature, signifying the formation of Vl-AgNP (Chinnasamy *et al.*, 2024).

Characterization of Al-AgNP

UV-visible spectroscopy analysis: The UV-visible spectra recorded in the wavelength range of 350-800 nm showed a distinct absorption peak at 435 nm which confirmed the formation of Vl-AgNPs (Fig. 3). This peak corresponded to the surface plasmon resonance (SPR) of AgNPs and indicated the reduction of Ag^+ to Ag^0 by the phytochemicals present in *V. leucoxylon* bark extract.

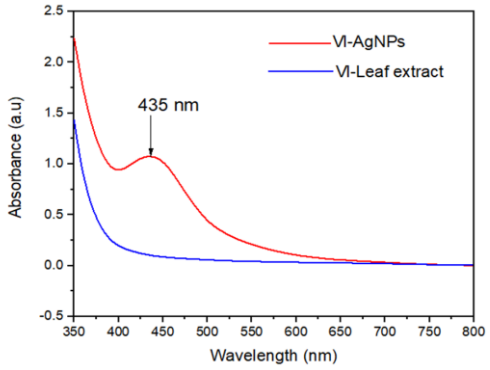

Fig. 3: UV-visible spectra of *Vitex leucoxylon* bark extract versus phytosynthesized AgNPs

FTIR analysis for Vl-AgNPs

FTIR analysis was performed to identify the functional groups involved in the reduction and stabilization of Vl-AgNPs. Fig. 4 presents the FTIR spectra of *V. leucoxylon* bark extract and the AgNPs synthesized from it. A prominent absorption peak at 3348.29 cm^{-1} was observed in the bark extract which corresponded to O-H stretching vibrations (Jiamboonsri *et al.*, 2021), indicating the presence of proteins, carbohydrates and polyphenols. Another band in *V. leucoxylon* aqueous bark extract was observed at 2936.25 cm^{-1} which indicated C-H bond stretching (Mukherjee *et al.*, 2002). Bands observed in *V. leucoxylon* bark extracts at 1609.02, 1441.58, and 1364.43 cm^{-1} corresponded to the aromatic ring vibrations and flavonoid's =C–O–C stretching (Jiamboonsri *et al.*, 2021). The band observed at 1077.97 cm^{-1} in *V. leucoxylon* bark extract is associated with C–O–C stretching vibrations related to carbohydrates (Katas *et al.*, 2019), while the band at 812.85 cm^{-1} corresponded to out-of-plane C–H bending vibrations. These results

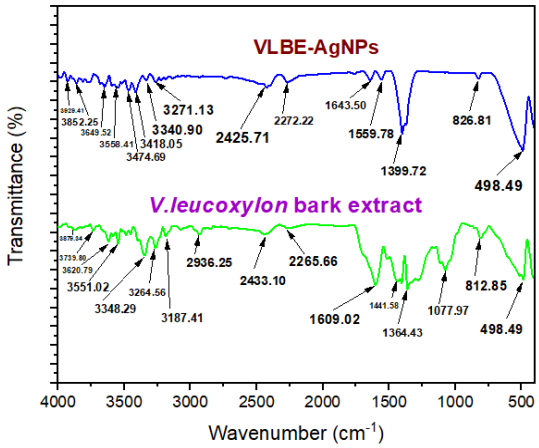

Fig. 4: FTIR spectra of *V. leucoxylon* bark extract and Vl-AgNPs

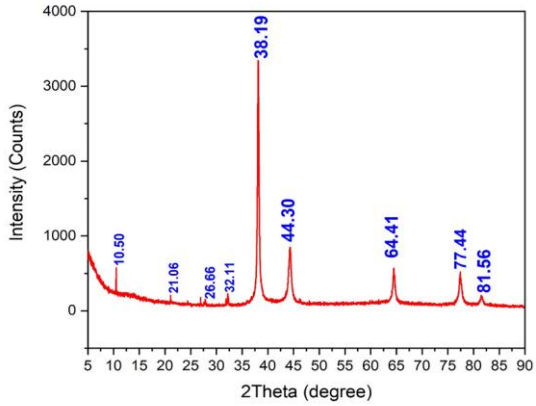

Fig. 5: XRD pattern for Vl-AgNPs

revealed that polyphenols played a major role in the reduction and capping of AgNPs from *V. leucoxylon* bark extract, while proteins and carbohydrates acted as stabilizing agents (Marslin *et al*., 2018). The FTIR spectra showed the functional groups of the molecules that have capping functions on the Vl-AgNP's surface. Vl-AgNPs spectra showed the characteristic infrared bands in *V. leucoxylon* bark extract, which were displaced and/or attenuated confirming that polyphenols and other phytochemicals in *V. leucoxylon* bark extract interact with AgNP surface for its stabilization. The near disappearance of band at 3348.29 cm^{-1} suggested the involvement of O-H groups in the reduction of Ag^{+} to Ag^{0}.

XRD analysis

The XRD pattern of Vl-AgNPs (Fig. 5) exhibited diffraction peaks at 2θ values of 38.19°, 44.30°, 64.41°, 77.44°, and 81.56°, which corresponded to (111), (200), (220), (311), and (222) planes of the face-centered cubic (FCC) structure of Vl-AgNPs (ICDD, 2001). These results confirm the crystalline nature and phase purity of the synthesized Vl-AgNPs. The most intense peak at (111) plane indicated the preferential orientation during nanoparticle formation.

Zeta potential and particle size analysis

The particle size distribution and zeta potential analysis of *V. leucoxylon* bark extract-mediated AgNPs are given in Fig. 6. The particle size of synthesized Vl-AgNPs ranged from 2.11 nm to 8510.56 nm, with highest particle density concentrated in the nanoscale region around the mean hydrodynamic diameter of 177.6 nm. The particle size distribution was evaluated using the polydispersity index (PDI); and a distribution is generally regarded as monodisperse when the PDI value is < 0.1. In present study, low polydispersity index (PDI = 0.09) was observed (Fig. 6a) which confirmed a narrow size distribution and monodisperse nature of nanoparticles, indicating uniform phytogenic synthesis. The intensity-based particle size distribution revealed that 54.53% particles were < 100 nm,

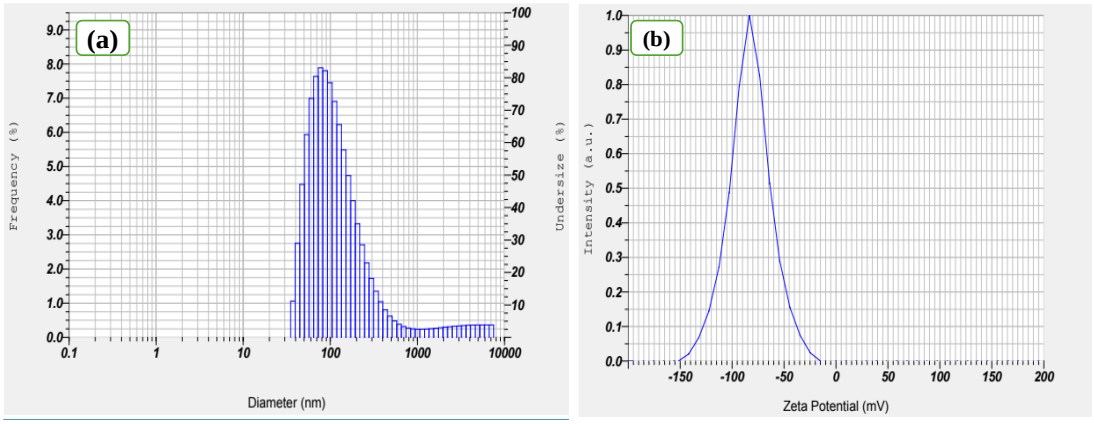

Fig. 6: Particle size distribution (a) and zeta potential (b) of Al-AgNPs

20.79% were in the range of 100-200 nm, and 24.68% were > 200 nm in size, confirming that the majority of particles fall within the nanoscale range.

Zeta potential reflects the surface charge and stability of nanoparticles. Zeta potential analysis (Fig. 6b) showed a single, sharp distribution peak with a high zeta potential value of −82.8 mV for Al-AgNPs, indicating strong electrostatic repulsion between particles (Mukherjee *et al*., 2014). The high negative surface charge confirms the excellent colloidal stability of Al-AgNPs and suggests effective capping of nanoparticles by phytochemicals present in the *V. leucoxylon* bark extract. The observed stability is consistent with the uniform particle density and low PDI obtained in the size distribution analysis.

SEM-EDX analysis

The surface shape of Al-AgNPs was examined by SEM, while the chemical elements present in the particles were identified and measured by EDX. SEM analysis revealed that phytosynthesized AgNPs were predominantly spherical with slight irregular agglomerations. The observed agglomerations may have occurred during sample drying before SEM examination since the TEM investigation indicated that the synthesized Al-AgNPs were uniformly distributed and predominantly spherical in shape (Fig. 8). EDX spectra showed a strong silver signal at 3 keV, confirming the presence of elemental silver (Fig. 7b). Other elements such as carbon, oxygen, and calcium showed weaker signals. These elements are among the substances found in plant extracts that stabilize AgNPs by binding to their surface and acting as capping agents (Gowda *et al.*, 2024).

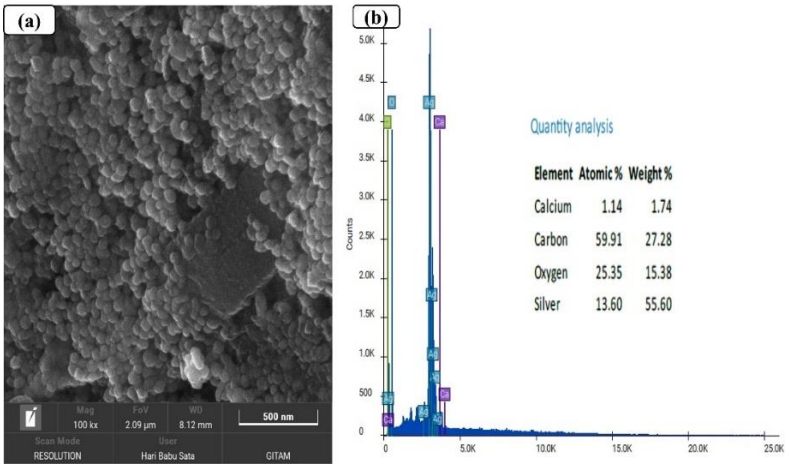

Fig. 7: SEM (a) and EDX (b) analysis of Vl-AgNPs

TEM analysis

TEM analysis revealed that Vl-AgNPs were nearly spherical to oval in shape with smooth surface morphology, with particle diameter ranging from 50.3 to 63.8 nm (Fig. 8). Similar observations have been reported for AgNPs synthesized by using *V. trifolia* leaf extract which showed spherical shape with a mean size of approximately 50 nm (Gowda *et al.*, 2024). The particle sizes determined by dynamic light scattering (DLS) were larger than those determined by TEM. This discrepancy is primarily because TEM measures the size of vacuum dehydrated particles, whereas DLS measures the hydrodynamic diameter, including surface-associated ions or molecules in the hydrated state in solution (Sudha *et al.*, 2017). The presence of phytochemicals

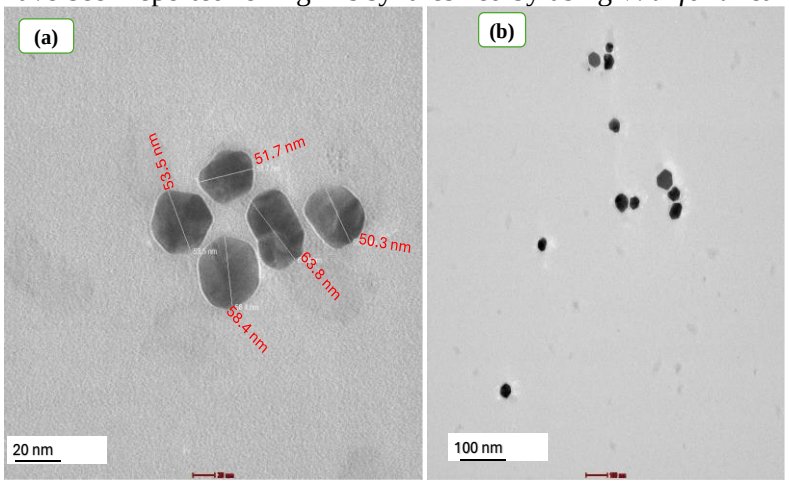

Fig. 8: TEM images of Vl-AgNPs with scale bars of (a) 20 nm and (b) 100 nm

including phenolic compounds appear to have contributed to the oval and spherical shape of Vl-AgNPs synthesized (Ahmed *et al*., 2016).

Phytochemical screening

The present study revealed the presence of phenols, flavonoids, phytosterols, saponins, steroids, alkaloids, anthocyanins, and terpenoids in the aqueous bark extract of *V. leucoxylon*; however, tannins and glycosides were absent. These phytochemicals have demonstrated anticancer, antiviral, anti-inflammatory, antibacterial, and antioxidant properties (Gavamukulya *et al*., 2014).

Antibacterial analysis of Vl-AgNPs

The antibacterial activity of phytosynthesized AgNPs was evaluated against *Bacillus coagulans*, *Pseudomonas aeruginosa*, *Staphylococcus aureus*, and *Escherichia coli* using the agar well diffusion method (Table 1; Fig. 9). Vl-AgNPs exhibited clear antibacterial activity against all test organisms, with inhibition zones showing increase in a concentration-dependent manner. Among the test bacteria, *E. coli* showed the highest susceptibility with a maximum inhibition zone of 22.1 ± 0.46 mm at the highest concentration of Vl-AgNPs. Moderate antibacterial activity was observed against *S. aureus* (19.2 ± 0.16 mm) and *B. coagulans* (18.4 ± 0.45 mm), whereas *P. aeruginosa* showed the lowest sensitivity with a maximum inhibition zone of 16.3 ± 0.36 mm. These results indicate that Vl-AgNPs are more effective against *E. coli* as compared to the other test bacteria. Based on the Kirby-Bauer disk diffusion assay and CLSI interpretative criteria (Chahardoli *et al*., 2022), Al-AgNPs demonstrated notable antibacterial efficacy against both G+ve and G-ve bacteria. The observed antibacterial activity may be attributed to the small size and surface characteristics of the synthesized Vl-AgNPs, which enhanced their interaction with bacterial cells, leading to the growth inhibition (Rai *et al.*, 2009).

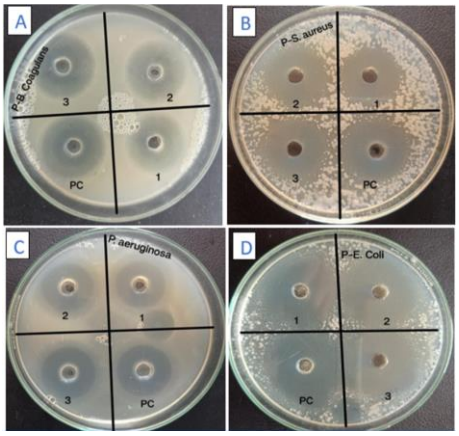

Fig. 9: Antibacterial activity of Vl-AgNPs against *Staphylococcus aureus* (A), *Bacillus coagulans* (B), *Pseudomonas aeruginosa* (C) and *Escherichia coli* (D)

Table 1: Antibacterial activity of AgNPs synthesized from aqueous bark extract of *V. leucoxylon*

Test organisms	Zone of inhibition (mm)			
	Al-AgNP (µg mL^{-1})			Standard*
	50	100	150	
Bacillus coagulans (MTCC-13124)	14.2 ± 0.96	16.2 ± 0.85	18.4 ± 0.75	20.1 ± 0.93
Staphylococcus aureus (MTCC-3160)	14.2 ± 1.16	16.2 ± 1.52	19.2 ± 2.16	21.2 ± 1.25
Pseudomonas aeruginosa (MTCC- 6363)	11.7 ± 0.16	13.5 ± 0.42	16.3 ± 0.36	18.2 ± 0.16
Escherichia coli (MTCC-443)	18.6±2.16	20.2 ± 2.22	22.1 ± 0.46	24.1 ± 2.12

*Chloramphenicol @ 30 µg mL^{-1}

Minimum inhibitory concentration

The test bacteria showed progressive decrease in growth with increase in the concentration of Vl-AgNPs. *E. coli* and *S. aureus* were more sensitive to the antibacterial action of Vl-AgNPs as they had lower minimum inhibitory concentration (MIC) than *P. aeruginosa* and *B. coagulans* (Fig. 10). After treatment with Vl-AgNPs at a specific concentration, no discernible growth occurred in test bacteria in broth cultures. The values for MIC of Vl-gNPs against *B. coagulans*, *E. coli*, *S. aureus*, and *P. aeruginosa* were 0.32, 0.80, 0.16, and 0.32 µg mL^{-1}, respectively (Table 2). At these MIC concentrations of Vl-AgNPs no discernible growth was observed in broth. A phytosynthesized AgNPs may be an efficient bactericidal agent as it prevents bacterial growth at low doses. Size of AgNPs determines how well they kill bacteria. Efficiency of a nanoparticle increases with decrease

in particle size. Following their passage through each bacterium's cell membrane, the generated nanoparticles attach to a variety of biomolecules which cause oxidative stress and eventually death of a cell (Chinnasamy *et al*., 2023).

Minimum bactericidal concentration (MBC)

The MBC was determined by culturing the aliquots from MIC dilution tubes onto MH agar plates to avoid misinterpretation caused by turbidity from insoluble compounds in the broth. When treated with Vl-AgNPs, the MBC values of *B. coagulans*, *S. aureus*, *P. aeruginosa*, and *E. coli* were 0.64, 0.32, 0.64, and 0.16, respectively (Table 2). The MBC completely prevented bacterial growth and was found to be higher than MIC (Fig. 10). Phytosynthesized AgNPs play a major role in antibacterial properties (Chinnasamy *et al*., 2023).

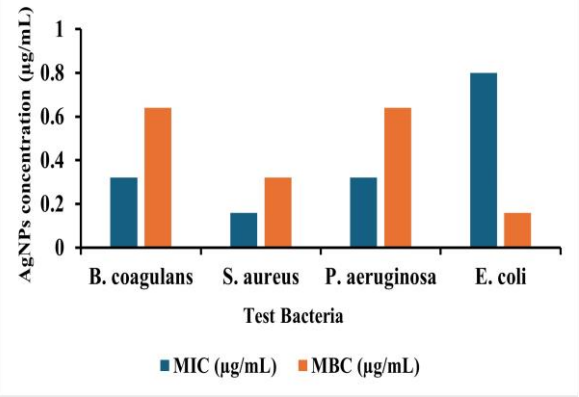

Fig. 10: Minimum inhibitory concentration (MIC) and minimum bactericidal concentration (MBC) for Vl-AgNPs

Table 2: MIC and MBC of Vl-AgNPs against test bacteria

Test organism	MIC (µg mL^{-1})	MBC (µg mL^{-1})
B. coagulans	0.32	0.64
S. aureus	0.16	0.32
P. aeruginosa	0.32	0.64
E. coli	0.80	0.16

In vitro antioxidant activity of Vl-AgNP

DPPH assay of Vl-AgNPs: The antioxidant activity of Vl-AgNPs was evaluated using the DPPH assay and compared with ascorbic acid as a standard (Fig. 11). Vl-AgNPs showed a concentration-dependent increase in the scavenging activity, rising from 11.8 ± 1.2% at 6.25 µg mL^{-1} to 77.42 ± 1.25% at 100 µg mL^{-1}. At concentrations between 12.5 and 50 µg mL^{-1}, Vl-AgNPs exhibited significantly higher scavenging activity than ascorbic acid. At 100 µg mL^{-1}, the difference between the two was reduced, which may be due to near-complete scavenging of available DPPH radicals, resulting in a saturation effect at higher concentrations (Prior *et al.*, 2005). The IC_{50} values were 20.06 µg mL^{-1} for Vl-AgNPs and 62.47 µg mL^{-1} for ascorbic acid, indicating comparable antioxidant potential. These results confirm that Vl-AgNPs possess strong dose-dependent free radical scavenging activity.

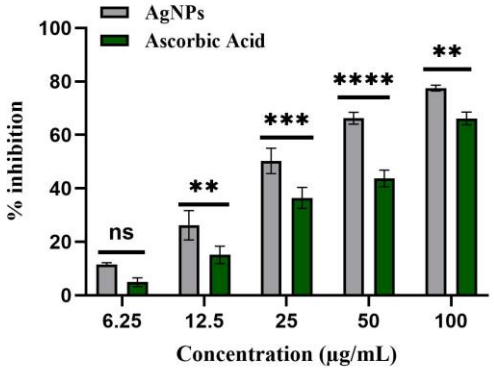

Fig. 11: DPPH assay of Vl-AgNPs. Error Fbar represents standard deviation of mean. *$p \leq 0.05$, **$p \leq 0.01$, ****$p \leq 0.0001$. Significant difference within a parameter between two lines is denoted by asterisk, and ns, means $p > 0.05$.

FRAP assay of Vl-AgNPs

In FRAP assay, both Vl-AgNPs and ascorbic acid showed a concentration-dependent increase in ferric reducing activity (Fig. 12). At the highest test concentration (50 µg mL^{-1}), ascorbic acid exhibited significantly higher reducing power (59.49 ± 1.60%) than Vl-AgNPs (35.67 ± 1.05%), indicating stronger electron-donating ability of standard antioxidant. However, Vl-AgNPs also demonstrated a consistent increase in reducing activity from 3.2 ± 0.8% at 10 µg mL^{-1} to 35.67 ± 1.05% at 50 µg mL^{-1}, confirming their notable antioxidant potential. The observed concentration-dependent FRAP activity of Vl-AgNPs is in agreement with previous reports on phytosynthesized AgNPs (Dua *et al.*,

2023). Chinnasamy *et al*. (2023) have reported high FRAP activity (90 ± 0.2%) for AgNPs synthesized using *Aristolochia bracteolata* bark extract at higher concentrations (100 µg mL^{-1}), suggesting that reducing power varies with plant source, phytochemical composition, and nanoparticle characteristics.

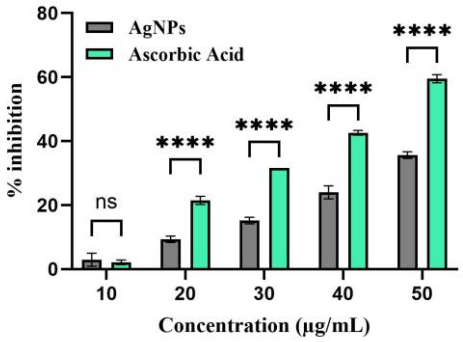

Fig. 12: FRAP assay of Vl-AgNPs. Error bar represents standard deviation of mean. *$p \leq 0.05$, **$p \leq 0.01$, ****$p \leq 0.0001$. Significant difference within a parameter between two lines is denoted by asterisk, and ns, means $p > 0.05$.

Cytotoxic activity of Vl-AgNP

Using colorimetric MTT test, the cytotoxicity of optimized Vl-AgNP was studied on HeLa cell line. The cell viability decreased in a concentration-dependent manner with increase in Vl-AgNP concentration (Fig. 13-14). Al-AgNP had IC_{50} values of 74.38 ± 0.31 µg mL^{-1} against HeLa cells. The findings suggest that biologically synthesised Vl-AgNPs have strong cytotoxical effects on the HeLa cancer cell line. The reduced size of Vl-AgNPs allowed them to pass through the cell wall by phagocytosis, pinocytosis, diffusion, or endocytosis. In cell, Vl-AgNPs lowered glutathione (GSH) levels and produced reactive oxygen species (ROS) which resulted in

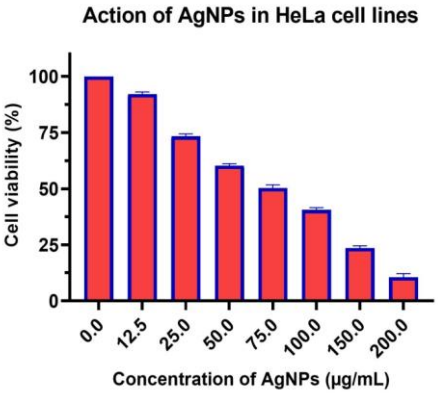

Fig. 13: *In vitro* cytotoxicity of phytosynthesized Al-AgNPs on HeLa cell lines

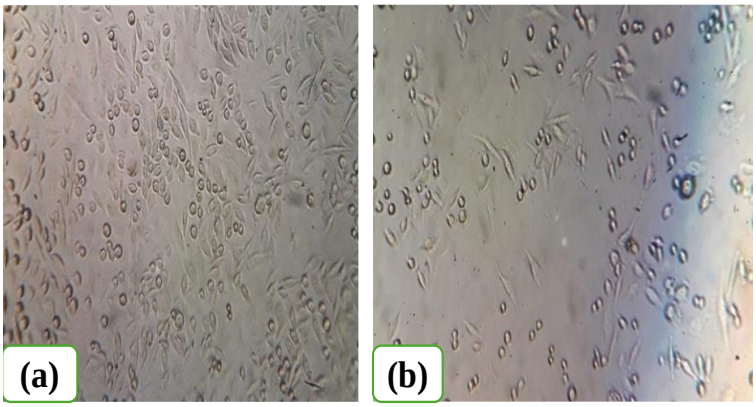

Fig. 14: Microscopic images of control cells (a) and cells treated with Vl-AgNPs at 150 µg mL^{-1} (b). [Images captured by using an inverted phase-contrast microscope at 200× magnification]

DNA destruction and eventually cell death due to the altered mitochondrial activities and stimulation of apoptotic genes (Barabadi *et al.*, 2020).

Conclusion: The study revealed that Vl-AgNPs were effectively produced using the aqueous bark extract of *Vitex leucoxylon* as both reducing and capping agents. Vl-AgNPs possessed a crystalline structure and display a characteristic surface plasmon resonance band at 435 nm. TEM revealed the synthesized AgNPs had average diameter of 50-64 nm. The biomedical efficacy of Vl-AgNPs was evident by their antioxidant, antibacterial, and anticancer capabilities. The Vl-AgNPs demonstrated notable antioxidant efficacy relative to the ascorbic acid standard used as standard. Consequently, Vl-AgNPs may serve as a promising component for the production of food and pharmaceuticals. Specifically, it may serve as a raw material in the drug development phase for conditions induced by excessive free radicals. Furthermore, Vl-AgNPs may facilitate the development of novel and more potent antibacterial and anticancer drugs. These findings suggest that Vl-AgNPs may serve as a potential solution to different health issues.

REFERENCES

Ahmed, S., Ahmad, M., Swami, B.L. and Ikram, S. 2016. A review on plants extract mediated synthesis of silver nanoparticles for antimicrobial applications: A green expertise. *Journal of Advanced Research*, **7**(1): 17-28.

Alzahrani, E., Ahmed, M.J., Ahmad, T. and Khan, M.A. 2021. Green synthesis of silver nanoparticles using *Teucrium polium* leaf extract: Characterization and antibacterial activity. *Materials Chemistry and Physics*, **258**(1): 123842. [*https://doi.org/10.1016/j.matchemphys.2021.123842*]

Barabadi, H., Vahidi, H., Damavandi Kamali, K., Rashedi, M. and Saravanan, M. 2020. Antineoplastic biogenic silver nanomaterials to combat cervical cancer: A novel approach in cancer therapeutics. *Journal of Cluster Science*, **31**(4): 659-672.

Chahardoli, A., Safaei, M., Mobarakeh, M.S., Fallahnia, N., Fatehi, B., Imani, M.M. *et al.*, 2022. Optimum green synthesis of silver nanoparticles with the highest antibacterial activity against *Streptococcus mutans* biofilm. *Journal of Nanomaterials*, **2022:** [*https://doi.org/10.1155/2022/6261006*].

Chinnasamy, R., Chinnaperumal, K., Arumugam, P., Natarajan, M., Govindasamy, B., Jogikalmat, K., *et al.*, 2024. Phyto-fabrication of AgNPs using leaf extract of *Vitex trifolia*: Potential to antibacterial, antioxidant, dye degradation, and their evaluation of non-toxicity to *Chlorella vulgaris*. *Biomass Conversion and Biorefinery*, **14**(13): 14903-14920.

Chinnasamy, R., Chinnaperumal, K., Cherian, T., Thamilchelvan, K., Govindasamy, B., Vetrivel, C., *et al.*, 2023. Eco-friendly phytofabrication of silver nanoparticles using aqueous extract of *Aristolochia bracteolata* Lam: Its antioxidant potential, antibacterial activities against clinical pathogens and malarial larvicidal effects. *Biomass Conversion and Biorefinery*, **14**(22): 28051-28066.

Cuendet, M., Hostettmann, K., Potterat, O. and Dyatmiko, W. 1997. Iridoid glucosides with free radical scavenging properties from *Fagraea blumei*. *Helvetica Chimica Acta*, **80**(4): 1144-1152.

DeGraff, W.G. and Mitchell, J.B. 1987. Evaluation of a tetrazolium-based semiautomated colorimetric assay: Assessment of chemosensitivity testing. *Cancer Research*, **47**(4): 936-942.

Dua, T.K., Giri, S., Nandi, G., Sahu, R., Shaw, T.K. and Paul, P. 2023. Green synthesis of silver nanoparticles using *Eupatorium adenophorum* leaf extract: Characterizations, antioxidant, antibacterial and photocatalytic activities. *Chemical Papers*, **77**(6): 2947-2956.

Gavamukulya, Y., Abou-Elella, F., Wamunyokoli, F. and AEl-Shemy, H. 2014. Phytochemical screening, anti-oxidant activity and *in vitro* anticancer potential of ethanolic and water leaves extracts of *Annona muricata* (Graviola). *Asian Pacific Journal of Tropical Medicine*, **7**(S1): S355-S363.

Gengan, R.M., Anand, K., Phulukdaree, A. and Chuturgoon, A. 2013. A549 lung cell line activity of biosynthesized silver nanoparticles using *Albizia adianthifolia* leaf. *Colloids and Surfaces B: Biointerfaces*, **105**: 87-91.

Gowda, A., Suman, T.C., Anil, V.S. and Raghavan, S. 2024. Phytosynthesis of silver nanoparticles using aqueous sandalwood (*Santalum album* L.) leaf extract: Divergent effects of SW-AgNPs on proliferating plant and cancer cells. *PLoS ONE*, **19**(4): 1-33.

Harborne, J.B. 1998. *Phytochemical Methods: A Guide to Modern Techniques of Plant Analysis* (3rd edn.). Springer, Dordrecht, The Netherlands.

ICDD. 2001. *PDF Card No. 04-0783: Silver (Ag)*. International Centre for Diffraction Data, Newtown Square, Pennsylvania, USA.

Jalilian, F., Chahardoli, A., Sadrjavadi, K., Fattahi, A. and Shokoohinia, Y. 2020. Green synthesized silver nanoparticle from *Allium ampeloprasum* aqueous extract: Characterization, antioxidant activities, antibacterial and cytotoxicity effects. *Advanced Powder Technology*, **31**: 1323-1332.

Jiamboonsri, P. and Wanwong, S. 2021. Photoassisted synthesis of silver nanoparticles using riceberry rice extract and their antibacterial application. *Journal of Nanomaterials*, **2021**: 1-18.

Katas, H., Lim, C.S., Nor Azlan, A.Y.H., Buang, F. and Mh Busra, M.F. 2019. Antibacterial activity of biosynthesized gold nanoparticles using biomolecules from *Lignosus rhinocerotis* and chitosan. *Saudi Pharmaceutical Journal*, **27**(2): 283-292.

Khan, I., Saeed, K. and Khan, I. 2019. Nanoparticles: Properties, applications and toxicities. *Arabian Journal of Chemistry*, **12**(7): 908-931.

Khan, M., Khan, M., Adil, S.F., Tahir, M.N., Tremel, W. and Alkhathlan, H. 2021. Green synthesis of silver nanoparticles using *Pulicaria glutinosa* extract: Characterization, antimicrobial and cytotoxic activity. *Colloids and Surfaces B: Biointerfaces*, **197**(2): 111331-111339.

Khutade, K., Dhinde, H., Kumari, N. and Shah, H. 2025. Comparative antibacterial activity of silver nanoparticles from *Blumea lacera* and *Neolamarckia cadamba* against methicillin-resistant *Staphylococcus aureus*. *Journal of Applied Biological Sciences*, **19**(1): 1-7.

Kumar, B., Smita, K., Cumbal, L. and Debut, A. 2020. Green synthesis of silver nanoparticles using *Andean blackberry fruit extract*: Characterization and antimicrobial activity. *Journal of Nanostructure in Chemistry*, **10**(3): 277-288.

Manimaran, K., Balasubramani, G., Ragavendran, C., Natarajan, D. and Murugesan, S. 2021. Biological applications of synthesized ZnO nanoparticles using *Pleurotus djamor* against mosquito larvicidal, histopathology, antibacterial, antioxidant and anticancer effect. *Journal of Cluster Science*, **32**(6): 1635-1647.

Manisha, M., Babu, R., Begam, A.M., Shakya Chahal, K. and Ashok Harale, A. 2025. Medicinal plants and traditional uses and modern applications. *Journal of Neonatal Surgery*, **14**(3): 162-175.

Marslin, G., Siram, K., Maqbool, Q., Selvakesavan, R.K., Kruszka, D., Kachlicki, P., *et al.*, 2018. Secondary metabolites in the green synthesis of metallic nanoparticles. *Materials*, **11**(6): [*https://doi.org/10.3390/ma11060940*]

Mukherjee, S., Chowdhury, D., Kotcherlakota, R., Patra, S., Vinothkumar, B., Bhadra, M. P., *et al.*, 2014. Potential theranostics application of bio-synthesized silver nanoparticles (4-in-1 system). *Theranostics*, **4**(3): 316-335.

Muthukrishnan, S., Chandrasekaran, G. and Pandiyan, J. 2025. Integrated GC-MS profiling, ADMET prediction, antibacterial and molecular docking studies of *Vitex leucoxylon* L.f. leaves extracts. *3 Biotech*, **15**(12): 445. [*https://doi.org/10.1007/s13205-025-04599-6*].

Prior, R.L., Wu, X. and Schaich, K. 2005. Standardized methods for the determination of antioxidant capacity and phenolics in foods and dietary supplements. *Journal of Agricultural and Food Chemistry*, **53**(10): 4290-4302.

Rai, M., Yadav, A. and Gade, A. 2009. Silver nanoparticles as a new generation of antimicrobials. *Biotechnology Advances*, **27**(1): 76-83.

Raja, A.S.A., Jebastin, N.S., Kaliappan, I. and Ramachandran, N. 2024. Green synthesis of three unique nanoparticles from *Hibiscus ficulneus* L. and assessment of their potential antimicrobial properties. *Applied Biological Research*, **26**(1): 33-42.

Sudha, A., Jeyakanthan, J. and Srinivasan, P. 2017. Green synthesis of silver nanoparticles using *Lippia nodiflora* aerial extract and evaluation of their antioxidant, antibacterial and cytotoxic effects. *Resource-Efficient Technologies*, **3**(4): 506-515.

Vinothkanna, A., Mathivanan, K., Ananth, S., Ma, Y. and Sekar, S. 2023. Biosynthesis of copper oxide nanoparticles using *Rubia cordifolia* bark extract: Characterization, antibacterial, antioxidant, larvicidal and photocatalytic activities. *Environmental Science and Pollution Research*, **30**(15): 42563-42574.

Wiegand, I., Hilpert, K. and Hancock, R.E.W. 2008. Agar and broth dilution methods to determine the minimal inhibitory concentration (MIC) of antimicrobial substances. *Nature Protocols*, **3**(2): 163-175.